

Ab initio Studies of the Possible Magnetism in BN Sheet by Non-magnetic Impurities and Vacancies

Ru-Fen Liu* and Ching Cheng†

Department of Physics, National Cheng Kung University, 70101, Tainan, Taiwan

We performed first-principles calculations to investigate the possible magnetism induced by the different concentrations of non-magnetic impurities and vacancies in BN sheet. The atoms of *Be*, *B*, *C*, *N*, *O*, *Al* and *Si* are used to replace either *B* or *N* in the systems as impurities. We discussed the changes in density of states as well as the extent of the spatial distributions of the defect states, the possible formation of magnetic moments, the magnitude of the magnetization energies and finally the exchange energies due to the presence of these defects. It is shown that the magnetization energies tend to increase as the concentrations of the defects decreases in most of the defect systems which implies a definite preference of finite magnetic moments. The calculated exchange energies are in general tiny but not completely insignificant for two of the studied defect systems, i.e. one with *O* impurities for *N* and the other with *B* vacancies.

PACS numbers: 75.75.+a, 73.22.-f, 67.57.Pq, 61.72.Ji

I. INTRODUCTION

The magnetism involving only *s*- and *p*-electron elements continues to attract much attention due to the potential of extensive applications as well as the urges to understand its physical origins. Recently, some experimental groups have discovered either weak or strong ferromagnetism in fullerenes[1, 2] and graphite[3] systems. A few theoretical studies attempting to find magnetism in some potential non-magnetic systems have also been carried out previously[4]. However, the origin of ferromagnetism in those systems is still under debate on both experimental and theoretical sides[1, 5]. The mechanism for forming magnetic ordering in solids, such as ferromagnetism, antiferromagnetism, etc., can be referred to the direct or indirect exchange interactions(super-exchange, double exchange, etc.) among magnetic moments. Therefore, a strong enough exchange interaction should be the crucial criterion to determine this possible new class of magnetic materials involving *s*- and *p*-electron atoms. In this work, the boron nitride(BN) sheet is used as the host system and the possible formation of magnetic moments by non-magnetic defects including substitutions of impurity atoms and creations of vacancies is studied. The exchange energies of those systems possessing finite magnetic moments are further examined and we shall demonstrate that there exist mostly very weak interactions among these defect-induced magnetic moments except two cases.

BN can form three different bulk structures which are hexagonal BN(h-BN), cubic BN(c-BN) and wurtzite BN(w-BN). Of these three structures, h-BN is the room temperature phase. Similar to graphite, h-BN is quasi-2D with weak interaction between layers. Nevertheless,

different from the delocalized π electrons in graphite, the stronger electronegativity of *N* than that of *B* causes π electrons to distribute more around *N*. This strong directional effect of bonding confine the motion of π -electrons and thus results in a gap in h-BN. BN is the lightest III-V compound of those that are isoelectronic with III-V semiconductors such as *GaAs*, but with wider band gap i.e. $E_g(BN) = 4.0 \sim 5.8$ eV at room temperature[6], compared with 1.42 eV of *GaAs*.

A 2D-structural material is usually a good basis for studying the physical properties of the most interesting nanostructures, such as nanotube, nano-ribbon etc.. The tubular structure of BN had been synthesized[7] experimentally. Moreover, it has been shown[8] that, in different ways of rolling up the BN nanotube, the electronic properties are all semiconducting which is the same as the extended BN sheet. This is very different from that of graphite and carbon nanotube which can be either metallic or semiconducting, depending on the way of rolling up. Therefore, one would expect that the effects of defects in BN sheet can catch many important physical properties as those would exist in the BN nanotubes.

In semiconducting and insulating systems, magnetic moments can be induced by defects[9, 10, 11]. Here, two different types of defects are used to study the possible formation of magnetic moments in BN sheet. One is that the atoms of *Be*, *B*, *C*, *N*, *O*, *Al* and *Si* are used to replace either *B* or *N* as impurities. The other is to create vacancies by removing either *B* or *N* atoms in BN sheet.

Our plans for this article are as the followings: Sec. II summarizes the computational methods in this work. The results of non-spin-polarized calculations are presented in Sec. III. In this section, the Subsec. A will present the electronic properties of BN sheet by the analyzed orbital-projected partial density of states (DOS). The Subsec. B includes the effects on DOS due to defects, i.e. the location of the defect states in DOS, as well as the extent of the spatial distribution of these defect states. All the results of spin-polarized calculations

*Electronic address: fmliu@phys.ncku.edu.tw

†Electronic address: ccheng@phys.ncku.edu.tw

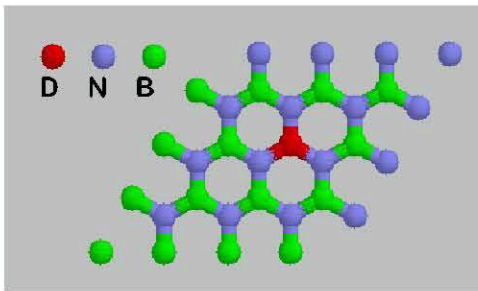


FIG. 1: (Color online) The 4×4 unit cell for the hexagonal BN sheet. D represents defects created in the system, i.e. impurities or vacancies.

are presented in Sec. IV. In the Subsec. A, we will investigate the possible formation of finite magnetic moments induced by defects while the results of exchange energies and the corresponding Curie temperatures will be presented in the Subsec. B. Finally, the conclusions are in Sec. V.

II. COMPUTATION METHOD

Our calculations are based on density functional theory(DFT)[12] with generalized gradient approximation(GGA) of Perdew and Wang[13] for the exchange-correlation energy functional. The PAW method[14] implemented by Kresse and Joubert[15] is used to describe the core-valence electrons interactions. There are 2, 3, 4, 5, 6, 3 and 4 valence electrons included here for Be , B , C , N , O , Al and Si respectively. The one-electron Kohn-Sham wavefunctions are expanded by the plane-wave basis with kinetic energy cut-off (E_{cut} hereafter) of 400 eV. The sampled k-points in the Brillouin zone(BZ) are generated by the Monkhorst-Pack technique[16] with gamma centered grids for hexagonal lattice. All calculations are carried out by Vienna *ab initio* simulation package(VASP)[17].

The calculated lattice constants of h-BN are $a = 2.5\text{\AA}$ and $c = 6.36\text{\AA}$ with $13 \times 13 \times 5$ k-point grids and compared with the experimental results($a = 2.5\text{\AA}$ and $c = 6.66\text{\AA}$)[18] are reasonably well[19]. The supercells composing of 4×4 primitive unit cells of BN sheet are used to simulate systems with defects(See FIG. 1). The vacuum distance between BN sheets (taken as along the z direction) was chosen to be around 13\AA which was tested with $3 \times 3 \times 1$ k-point grids to be large enough to avoid interactions between the sheets.

Of all the relaxed configurations in this work, the atomic forces calculated by Hellmann-Feynman theorem[21] were smaller than 0.02 eV/\AA . In the spin-polarized calculations, we performed the above atomic relaxations again to ensure the relaxed configurations. The DOS and magnetic moments of the final relaxed structures were then evaluated. The larger supercells of 8×4 and 8×8 were used to study the possible finite magnetic

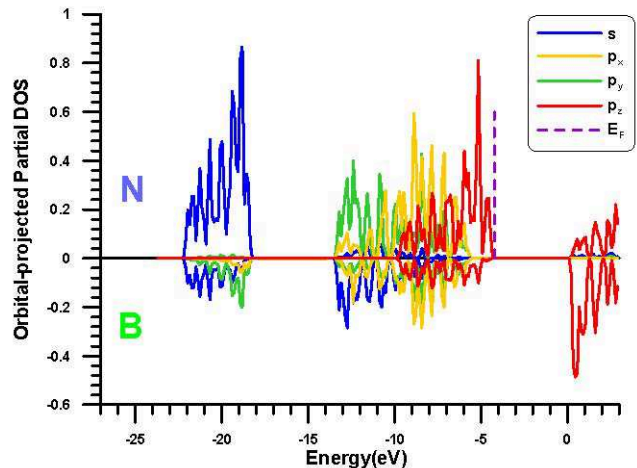


FIG. 2: (Color online) The orbital-projected partial density of states for N and B atoms in hexagonal BN sheet.

moments induced by defects, as well as the variation of the magnetization energy (denoted as E_M hereafter) and the exchange energy J with respect to the distances between defects, i.e. defect concentrations.

III. NON-SPIN-POLARIZED CALCULATIONS: DENSITY OF STATES

A. BN sheet

The orbital-projected partial DOS of B and N in BN sheet are presented in FIG. 2. The colors of blue, yellow, green and red in the figures represent the s -, p_x -, p_y - and p_z -orbital-projected partial DOS respectively. The spiky feature of the DOS is due to the dimensional reduction from 3D bulk h-BN to 2D planar structure of BN sheet. Two valance bands (shorted as VB hereafter) and the lowest 3eV range of the conduction band (shorted as CB hereafter) are included in the figure for discussion. The DOS's in the same energy range for BN sheets with defects will be used in the following discussion for comparison and the bottom of the CB is taken as the zero of the energy for convenience in discussing the splitting of the electronic bands from the two VBs as well as the CB due to the presence of defects. The two VBs in BN sheet are well-separated as those in the bulk h-BN[18]. The lower-energy VB (VB1 hereafter) contains 2 electrons: one is from the s -electron of N and the other is from the hybridized s - and p -electrons (sp^2 -electrons hereafter) of B . The higher-energy VB (VB2 hereafter) contains 6 electrons, i.e. three sp^2 -electrons and one p_z -electron from N and two sp^2 -electrons from B . From FIG.2 we see that the nature of the two VBs for B is mainly hybridized sp^2 -orbitals while that for N is s -like orbitals in VB1 and hybridized sp^2 -like orbitals in VB2. Near the top of VB2 and the bottom of CB, the DOS's are mostly p_z -orbital

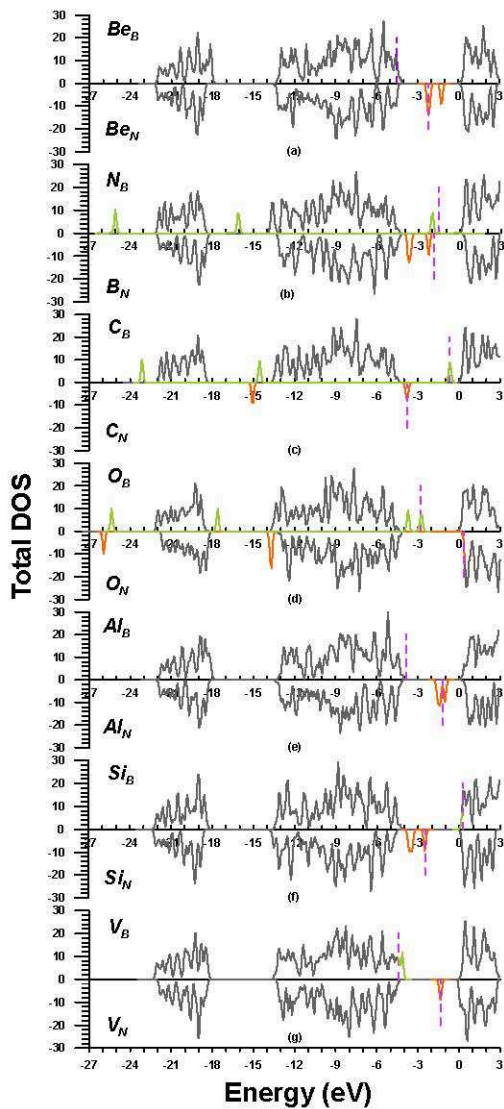


FIG. 3: (Color online) The DOS's for the BN sheet with defects. The upper panel shows defects on B while the lower one shows defects on N . (a)-(f) are the results of the defect systems with impurities Be , N , B , C , O , Al and Si atoms respectively. The defect systems with B and N vacancies are shown in (g). All dashed lines cut at E_F .

in nature. However, the dominant contribution switches from the p_z -orbital on N atoms near the top of VB2 to the p_z -orbital on B atoms near the bottom of CB. That is the electronic excitation in BN sheet would involve displacement of electron distribution from the p_z -orbital around N atoms to the p_z -orbital around B atoms.

B. Effect of defects

In the present section, we discuss the effect of defects on the DOS of BN sheet when the spin-polarization is not yet switched on. We shall demonstrate that the ef-

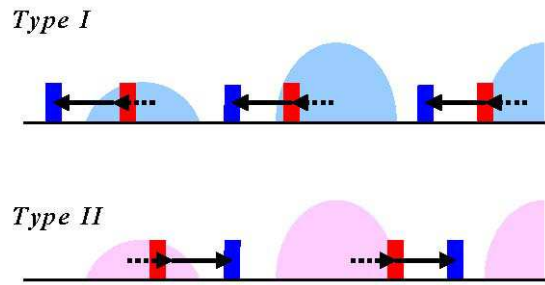


FIG. 4: (Color online) Schematic diagrams of the effect of defects on DOS. The dashed lines show the possible circumstances in forming metal-like DOS.

fect of defects on the DOS can be generally categorized into two groups according to the chemical properties of the defects. The 4×4 supercell was employed in all the results presented in this section which corresponds to a doping of $1/32$ ($\sim 3\%$) of the defects in the system and a distance of 10.03\AA between the neighboring defects. The possible interaction between defects will be discussed in the following section when the exchange energy is investigated. However, the results presented in the present section are applicable to the systems with low-density dopings of defects as we shall demonstrate in the following section that the interaction between defects is already quite small in the present configurations. The effect of C impurity on the DOS of BN sheet will be discussed in details first and then followed by the results for the series of defects we studied. For simplicity, we denote, e.g. C_B , as the defect system which consists of an impurity of C atom substituting one of B atoms in the original supercell of BN sheet and $V_B(V_N)$ as the system consisting of a vacancy replacing one of the original $B(N)$ atoms.

One of the effects of the impurities is to introduce electronic states into the energy regions which originally have no DOS in the BN sheet. We present the total DOS of all the defect systems considered in this study in FIG.3. In the case of C_B (FIG.3(c)), the defect states split from the original three bands and move to the lower energy region. This is due to the stronger bonding ability of C ions for electrons compared to that of B ions. On the contrary, in the case of C_N , the bonding ability of C ion is weaker than that of N ion for electrons such that the defect bands move to the higher-energy positions compared to the original three bands. Therefore, the locations of defect bands is determined by the bonding ability of the defects compared to the substituted host atoms. The effects of defects on the DOS's can be summarized into two types as outlined schematically in FIG.4. For N_B , C_B , O_B , O_N and Si_B , the bonding abilities of the impurities are stronger than the substituted host atoms. We name these as type I. For Be_B , Be_N , B_N , C_N , Al_N and Si_N , which are named as type II, the three defect bands all move to the region of higher energy than the original three bands.

Of these studied defect systems, some consist of odd

number of electrons in the supercell, i.e. Be_B , Be_N , C_B , C_N , O_B , O_N , Si_B , Si_N , V_B and V_N , such that there is an unpaired electron occupying the defect state located between the VB2 and CB for Be_N , C_B , C_N , O_B , Si_N and V_N , the top of VB2 for Be_B and V_B as well as the bottom of CB for O_N and Si_B . We denote DB as the state that the unpaired electron occupies hereafter. We shall show in the next section that magnetic moments are likely to form for those cases with partially occupied DBs. In case the partially occupied defect bands which form definite magnetic moments are also extended in nature, the long-range magnetic order can develop. Hence, it is expected that for Be_B , O_N , Si_B and V_B whose defect states locating at the edge of the original extended bands, the defect bands are more likely to be extended in nature and then more likely to lead to larger exchange energies as will be presented in the next section.

In order to determine the properties of the partially-filled DBs, the extent of the states in space is established from summing over the contributions of the orbital-projected partial DOS of the DBs for the neighboring atoms of the defects as presented in FIG.5. For Be_B , Be_N , O_B and O_N , we see that the electrons of the DBs distribute more on the nearest neighboring atoms of the impurity than the impurity itself. This is contrary to the C_B , C_N , Si_B and Si_N systems in which most of the electrons of the DBs distribute around the impurity atoms. These results demonstrate that the electrons of the defect states due to impurities do not have to distribute mostly on the impurities themselves. About the spatial extent of the defect states, FIG.5 shows that only three systems, i.e. Be_B , O_N and V_N , reach beyond 5\AA . However, the defect states for all the defect systems considered in the present study are confined in a distance of 6\AA around the defects no matter whether the partially-filled defect states are at the edge of the extended bands or not. Finally, we should emphasize that FIG.5 also reveals two categories of DBs: one is formed by the sp^2 -hybridized orbitals, e.g. s , p_x and p_y , and the other is p_z in nature. These orbital-projected-DOS analyses imply the difference of the electronic distributions of the magnetic moments (detail discussions in the next section) formed by the unpaired electrons in DB, e.g. the moments are distributed on the plane of BN sheet for Be_N , O_B and V_B while the moments are distributed perpendicularly to the plane of BN sheet for Be_B , C_B , C_N , O_N , Si_B , Si_N and V_N systems.

IV. SPIN-POLARIZED CALCULATIONS: THE EFFECTS OF DEFECTS

In this section, we present the results of spin-polarized calculations to investigate the possible formation of finite magnetic moment in the BN sheets containing defects as well as the possible long-range magnetic ordering in these systems.

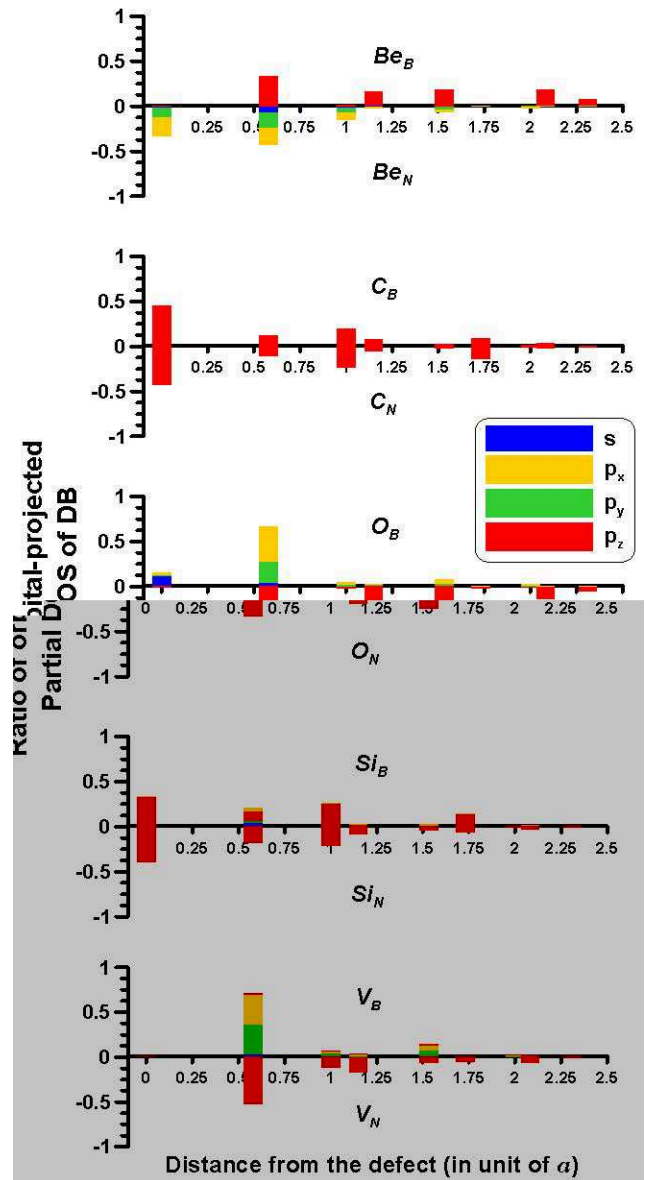


FIG. 5: (Color online) The ratio of the orbital-projected partial DOS summing over the i th nearest neighbours of the defect of the system with partially-filled DB. There are 1(the defect), 3, 6, 3, 6, 6, 3, 3 and 1 atoms contributing to each bars in sequence. a is the lattice constant 2.5\AA .

A. The possible formation of magnetic moments

To identify the possible magnetic moments due to defects as well as the extent of the magnetic moments, the 4×4 and 8×8 supercells consisting of only one defect were employed to simulate the BN sheet with defect concentrations of 3.125% and 0.78% respectively, i.e. corresponding to a distance of 10.03\AA and 20.05\AA between nearest-neighbour defects (denoted by d_D hereafter). In order to obtain the relevant physical quantities for the cases within the range between $d_D = 10\text{\AA} \sim 20\text{\AA}$, we create a rectangular supercell as shown in FIG.6. By

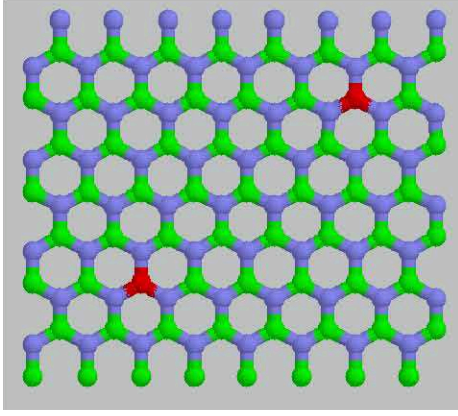


FIG. 6: (Color online) The rectangular supercell with cell dimensions 20.05\AA and 17.37\AA . The distance between the two defect sites is 13.26\AA . The supercell contains 64 primitive cells of BN sheet.

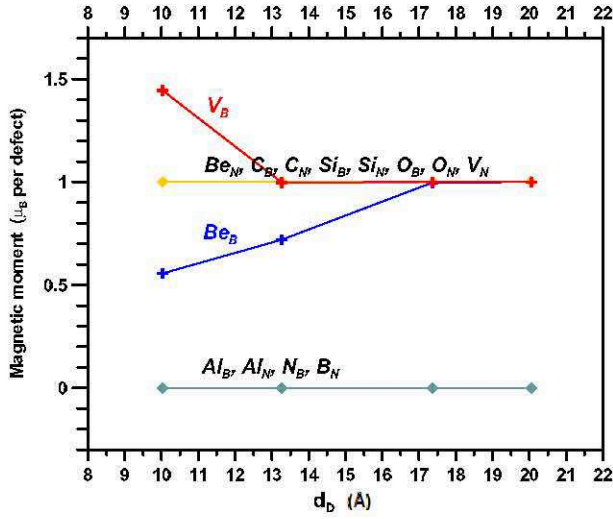


FIG. 7: (Color online) The calculated magnetic moments with respect to d_D , the distance between the nearest-neighboring defects.

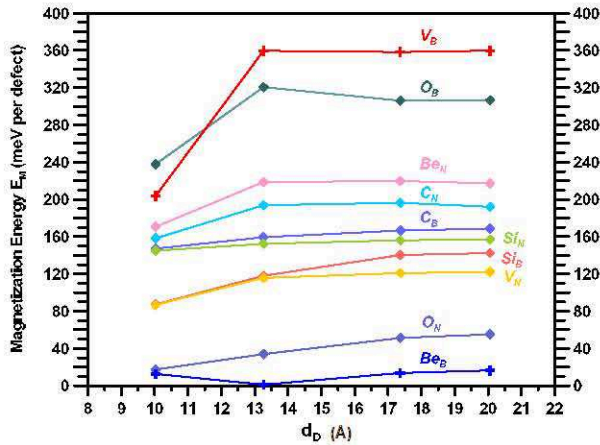


FIG. 8: (Color online) The magnetization energy E_M v.s. d_D .

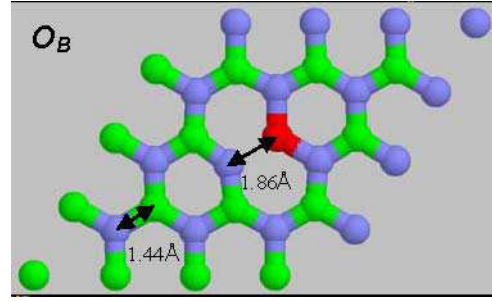


FIG. 9: (Color online) The relaxed structure for the defect system of O_B . The impurity, O atom, was relaxed and moved toward two of the three neighboring N atoms to open up one of the original $N - O$ bonds. The spin-polarized energy for this configuration with unequal $N - O$ bond lengths is lower than that with equal $N - O$ bond lengths by 111meV .

providing either one defect or both defects in the supercell of FIG.6, one can simulate the cases of 17.37\AA and 13.26\AA for d_D respectively. The calculated magnetic moments of the systems with respect to d_D are presented in FIG.7. For N_B , B_N , Al_B and Al_N which have even number of electrons in the supercell and completely-filled DBs, there exist no magnetizations and they are therefore excluded from the following discussions. The calculated magnetic moments in Be_B and V_B were found to vary as d_D increases. However, their magnitudes converge to $1\mu_B$ as d_D increases to 17.37\AA . For Be_N , C_B , C_N , O_B , O_N , Si_B , Si_N and V_N , the calculated magnetic moments are always found to be $1\mu_B$ and independent of d_D . Note that for all the defect systems possessing finite magnetic moments, the defect bands are always partially occupied. The $1\mu_B$ of magnetizations in these defect systems should be attributed to the unpaired electron occupying the defect states.

To understand how stable these finite moments in BN sheet are, the magnetization energies, i.e. E_M , obtained from the total-energy difference between the systems with and without spin-polarized configuration were calculated. The results are plotted in FIG.8. Firstly, the E_M s of these systems tend to increase as d_D s increase. This suggests a definite preference of finite magnetic moments for these defect systems with distant non-magnetic defects. Secondly, the corresponding E_M for these defect systems with distant defects can be determined by the saturated values in the figure, e.g. 360meV for V_B , 300meV for O_B , 220meV for Be_N etc., and then are found to be in the wide energy distribution (from 16meV of Be_B to 360meV of V_B). We notice that the defect systems with metal-like electronic properties (Be_B , O_N , Si_B and V_B), i.e. with fermi level at the edge of either VB2 or CB, do not necessarily lead to large E_M . For example, the E_M of Be_B is very small, i.e. 16meV which is even smaller than the room temperature thermal energy of 25meV . However, the E_M of V_B is the largest, i.e. 360meV , of all the systems we considered. We should mention that, when the defect distance is increased, the

metal-like DOS does not always hold. The bandwidth of the defect bands might become smaller due to localization such that they eventually separate from the original VB2 or CB bands. Of the studied systems with metal-like DOS at $d_D = 10.03\text{\AA}$, this happens in Si_B and V_B whose defect bands are originally at the edge of CB and VB2 respectively. For Be_B and O_N , the defect bands remain at the edge of VB2 and CB respectively up to the largest $d_D = 20.05\text{\AA}$ we studied.

Finally, for those systems with p_z -like magnetic moments, the bond lengths between defect and neighboring host atoms were found relaxed but preserving the three-fold symmetry. However, we found that, the relaxed bond lengths of Be_N , O_B and V_B which have planar distributions in the magnetic moments (the sp^2 -hybridized electron in DB) undergo structural distortions and break the three fold symmetry of the original BN systems after the spin-polarization calculation is switched on (John-Teller(JT) effect). FIG.9 shows the relaxed structure of O_B . The impurity, O atom, moved toward two of the neighboring N atoms to open up one of the three original $N - O$ bonds. The total energy of this distorted structure with spin-polarization is lower than that of the structure with equal $N - O$ bond length by 111meV, similarly for Be_N by 33meV and for V_B by 47meV. The effect of JT distortion are also responsible for the consequences of relatively larger magnetization energy of Be_N , O_B and V_B with planarly distributed moments compared to those with p_z -like moments.

B. The exchange energy

From the above analyses, we have demonstrated that the non-magnetic defects can induce finite magnetic moments in BN sheet. To identify the possible long-range magnetic ordering in these systems, the Heisenberg-type of spin couplings[22] is employed to model the interaction (J , i.e. the exchange energy) between the nearest-neighbor magnetic moments due to defects. The exchange energy J is determined from the total-energy difference between two spin configurations, i.e. one with antiparallel and the other with parallel spin configuration whose energy are denoted as E_{AFM} and E_{FM} respectively hereafter. For simulating two defects distancing 10.03\AA , we employed either the 8×4 supercell with two defect sites in each sub-supercells of 4×4 or the 8×8 supercell with those in the two diagonal sub-supercells of 4×4 to generate different spin configurations. In the antiferromagnetic configuration, the 8×4 supercell describes a configuration of six nearest neighbours ($d_D = 10.03\text{\AA}$) in which four are antiparallel- and two are parallel-spin to the centered defect while the 8×8 supercell describes a configuration of two antiparallel-spin nearest neighbours ($d_D = 10.03\text{\AA}$) and a $d_D = 17.37\text{\AA}$ for the four next-nearest neighbours. The rectangular supercell in FIG.6 with defects on both sites is also used to simulate the two spin configurations for the systems with defect distance of

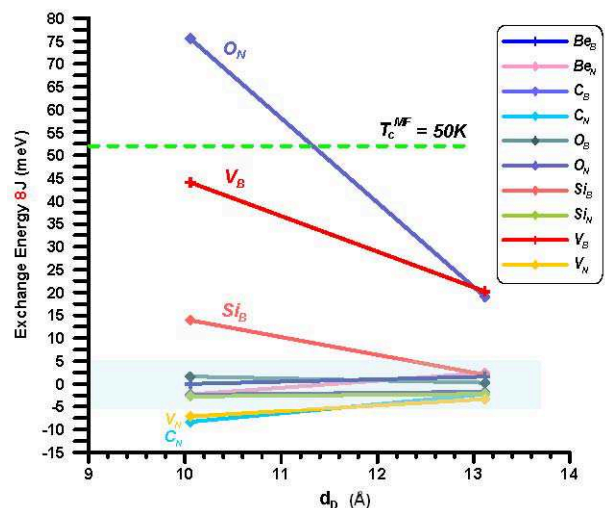


FIG. 10: (Color online) The exchange energy $8J$ v.s. defect distances where $J \equiv \frac{1}{8}\{E_{AFM} - E_{FM}\}$. The energy range from -5meV to 5meV is the estimated region where the magnitude of $8J$ is too small to be used to identify the sign of $8J$ in our calculations. The dashed line indicates the value of exchange energy respected to 50K of Curie temperature (T_c^{MF}) under mean-field approximation.

13.26\AA . In the rectangular supercell, there are four nearest neighbours for a defect and all are antiparallel-spin neighbours in the antiferromagnetic configuration. We have used both 8×4 and 8×8 supercells for the V_B and O_N systems and the exchange energy obtained from the 8×8 supercells were considered in the discussion as they correspond more to the low-doping conditions we would like to consider. The different values of the exchange energies obtained from using 8×4 and 8×8 supercells indicate that the simple pair-wise Ising interaction is not a good enough model to describe the energies of these systems of $d_D = 10.03\text{\AA}$. We notice that both V_B and O_N have DB at the edge of either CB or VB2. The 8×8 supercells were also used on a few of the other defect systems, but all lead to similar results as those obtained from the 8×4 supercells.

Our results are summarized in FIG.10 where the lines are to guide the eyes. From the previous magnetization energy calculations, our computational accuracy can recognize meaningful energy difference of 5meV and larger values between configurations. For those systems of Be_B , Be_N , C_B , O_B and Si_N , the calculated $8Js$ which are less than 5meV are too small to determine whether the systems are ferro- ($8J > 0$) or antiferromagnetic ($8J < 0$). For O_N , V_B and Si_B , they are found to be ferromagnetic, and for C_N and V_N , anti-ferromagnetic at $d_D = 10.03\text{\AA}$. We should mention that the relaxed spin configurations of all the systems discussed here remained anti-ferromagnetic at the end of the calculations if with initial antiparallel-spin configurations. The exchange energies for O_N , V_B and Si_B , which possess metal-like DOS, are relatively larger at $d_D = 10.03\text{\AA}$, but not for

the case of Be_B whose E_M is tiny anyway. Although the magnetization energy of V_B can be as large as 200meV at $d_D = 10.03\text{\AA}$, the exchange energy is considerably much smaller (5.6meV), similarly for Si_B whose $E_M \sim 90meV$ while J is smaller than 2meV. (Note FIG.10 shows the data of 8 times the exchange energy J .) This contrast is much reduced in the case of O_N whose $E_M \sim 17meV$ and $J \sim 9.4meV$ at $d_D = 10.03\text{\AA}$. When the d_D is increased to 13.26\AA, the magnitude of exchange energies for all the above systems decrease. At the end, there are only two systems, i.e. O_N and V_B , which have large enough exchange energies to be identified numerically as the magnetically ordered systems.

Within the framework of Heisenberg spin model, it is possible to estimate the Curie temperatures (T_c) of these systems. The mean-field result is given by

$$k_B T_c^{MF} = \frac{2}{3} \bar{J}_0, \quad (1)$$

where \bar{J}_0 is the on-site exchange parameter reflecting the exchange field created by all the neighbouring magnetic moments[23, 24]. Note that the T_c determined by Eq.(1) is regarded as an overestimated values[25]. Since the physics of T_c involves the disorder nature of the system due to temperature, \bar{J}_0 should be related to the energy difference between the local disorder state and ferromagnetic state of the system[24]. However, the exchange energies obtained here do not include disorder effect, i.e. E_{AFM} is calculated from ordered anti-ferromagnetic configuration. Hence, the estimated T_c (denoted as \tilde{T}_c^{MF} hereafter) by just simply substituting J in FIG.10 into the \bar{J}_0 in Eq.(1) is expected as an upper-bound of T_c^{MF} for a given system. For O_N , V_B and Si_B with relatively large J s at $d_D = 10.03\text{\AA}$, the \tilde{T}_c^{MF} s are 72K, 43K and 13K respectively. However, they reduce to around 20K for O_N and V_B , below 5K for Si_B when d_D is increased to 13.26\AA. In addition, the \tilde{T}_c^{MF} s of the defect systems with exchange energies smaller than 5meV are all below

5K in different concentrations. Therefore, one can conclude that the effect of the long-range magnetic ordering is very weak in all the defect systems considered here except for the defect systems of O_N and V_B . However, our calculations suggest that the systems of Be_N , C_B , C_N , O_B , O_N , Si_B , Si_N , V_B and V_N all have finite magnetic moments and are therefore at least paramagnetic.

V. CONCLUSIONS

Different concentrations of non-magnetic impurities and vacancies in BN sheet were studied using first-principles methods to investigate the possible magnetism in these systems involving only s - and p -electron elements. We firstly studied the effects of these defects on DOS and analyzed the characters as well as the spacial extent of these defect states. The magnetization energies, possible magnetic moments as well as the exchange energies for these defect systems in different concentrations were evaluated. We demonstrated that all the defect systems with partially-filled defect bands exhibited a definite preference for finite magnetic moments. The calculated exchange energies for low-density defect systems are all tiny except for the O_N and V_B whose exchange energies are not completely insignificant with an estimated T_c of 20K.

Acknowledgments

This work was supported by the National Science Council of Taiwan. Part of the computer resources are provided by the NCHC (National Center of High-performance Computing). We also thank the support of NCTS (National Center of Theoretical Sciences) through the CMR (Computational Material Research) focus group.

-
- [1] T. L. Makarova et al., Nature(London), **413**, 716 (2001); However, retraction in T. L. Makarova et al., Nature(London), **440**, 707 (2006) and references within.
- [2] M. Tamura et al., Chem. Phys. Lett. **186**, 401 (1991); P. M. Allemand et al., Science, **253**, 301 (1991); Y. Murakami and H. Suematsu, Pure Appl. Chem. **68** 1463, (1996); F. J. Owens, Z. Iqbal, L. Belova, K. V. Rao, Phys. Rev. B **69**, 033403 (2004); O. E. Kvyatkovskii, I. B. Zakharova, A. L. Shelankov, T. L. Makarova, Phys. Rev. B **72**, 214426 (2005).
- [3] P. Esquinazi et al., Phys. Rev. B **66**, 024429 (2002) and Phys. Rev. Lett., **91**, 227201 (2003); Y. Kopelevich et al., J. Low Temp. Phys., **119**, 691 (2000).
- [4] Yong-Hyun Kim, J. Choi, K. J. Chang, D. Tomanek, Phys. Rev. B **68**, 125420 (2003); Yuchen Ma et al., New J. Phys. **6** 68, (2004); H. J. Xiang et al, New J. Phys., **7**, 39 (2005); Hong Seok Kang, J. Phys. Chem. B **110**, 4621 (2006); R. Q. Wu et al., J. Phys.: Condens. Matter **18** 569 (2006); M. S. Si and D.S.Xue, Europhys. Lett., **76**(4), 664 (2006).
- [5] A. N. Andriotis, M. Menon, R. M. Sheetz, L. Chernozatonskii, Phys. Rev. Lett., **90**, 026801 (2003); P. Esquinazi et al., Phys. Rev. Lett., **91**, 227201 (2003); P. O. Lehtinen, A. S. Foster, Y. Ma, A. V. Krasheninnikov, R. M. Nieminen, Phys. Rev. Lett., **93**, 187202 (2004).
- [6] S. L. Rumyantsev et al., in "Properties of Advanced Semiconductor Materials GaN, AlN, InN, BN, SiC, SiGe". Edited by M. E. Levinstein, S. L. Rumyantsev, M. S. Shur, John Wiley and Sons, Inc., New York, 2001, p67-92.
- [7] J. Cumings and A. Zettl, Chem. Phys. Lett. **316**, 211 (2000); E. Bengu and L. D. Marks, Phys. Rev. Lett., **86**, 2385 (2001); W. Mickelson, S. Aloni, W. Han, J. Cumings, and A. Zettl, Science **300**, 467 (2003); F. F.

- Xu, Y. Bando and D. Golberg, *New J. Phys.* **5** 118 (2003).
- [8] X. Blase, A. Rubio, S. G. Louie, and M. L. Cohen, *Europhys. Lett.* **28**, 335 (1994).
- [9] J. Osorio-Guillén, S. Lany, S. V. Barabash, A. Zunger, *Phys. Rev. Lett.*, **96**, 107203 (2006).
- [10] D. M. Edwards and M. I. Katsnelson, *J. Phys.: Condens. Matter* **18**, 7209 (2006).
- [11] A. N. Andriotis, R. M. Sheetz and M. Menon, *J. Phys.: Condens. Matter* **17** L35-L38 (2005).
- [12] P. Hohenberg and W. Kohn, *Phys. Rev.*, **136**, B864 (1964); W. Kohn and L. J. Sham, *Phys. Rev.*, **140**, A1133 (1965).
- [13] J. P. Perdew in *'Electronic Structure of Solids '91*, edited by P. Ziesche and H. Eschrig (Akademie-Verlag, Berlin, 1991); J. P. Perdew et al., *Phys. Rev. B* **46**, 6671 (1992).
- [14] P.E. Blöchl, *Phys. Rev. B* **50**, 17953 (1994).
- [15] G. Kresse and D. Joubert, *Phys. Rev. B* **59**, 1758 (1999).
- [16] H. J. Monkhorst and J. D. Pack, *Phys. Rev. B* **13**, 5188 (1976).
- [17] G. Kresse and J. Hafner, *Phys. Rev. B* **47**, 558 (1993); **49**, 14251 (1994); G. Kresse and J. Furthmüller, *Comput. Mater. Sci.* **6**, 15 (1996); *Phys. Rev. B* **54**, 11169 (1996).
- [18] N. Ooi, A. Rairkar, L. Lindsley and J. B. Adams, *J. Phys.: Condens. Matter* **18** 97 (2006).
- [19] The lattice constants calculated from LDA with $E_{cut} = 400\text{eV}$ are $a = 2.48\text{Å}$ and $c = 5.9\text{Å}$ and become $a = 2.5\text{Å}$ and $c = 6.23\text{Å}$ when E_{cut} is increased to 500eV . However, the GGA results of c become 7Å at $E_{cut} = 500\text{eV}$. Similar results of overestimation for c in hexagonal BN from GGA has been documented in [18, 20].
- [20] A. Janotti, S.-H. Wei and D. J. Singh, *Phys. Rev. B* **64**, 174107 (2001).
- [21] H. Hellmann, *Einführung in die Quantenchemie* (Deuticke, Leipzig, 1937), pp.61 and 285; R. P. Feynman, *Phys. Rev.* **56**, 340 (1939).
- [22] With Heisenberg Hamiltonian: $H = -2J \sum_{ij} \mathbf{S}_i \cdot \mathbf{S}_j$, we have $\xi J \equiv E_{AFM} - E_{FM}$, where ξ is effective coupling pairs.
- [23] K. Sato, P. H. Dederics and H. Katayama-Yoshida, *Europhys. Lett.*, **61**(3), 403 (2003).
- [24] J. Kudrnovský et al., *Phys. Rev. B* **69**, 115208 (2004).
- [25] G. Bouzerar, T. Zinman and J. Kudrnovský, *Europhys. Lett.*, **69**(5), 812 (2005).